

High-pressure behaviour of $\text{Li}_2\text{CaHfF}_8$ scheelite

This article has been downloaded from IOPscience. Please scroll down to see the full text article.

2007 J. Phys.: Condens. Matter 19 096215

(<http://iopscience.iop.org/0953-8984/19/9/096215>)

View [the table of contents for this issue](#), or go to the [journal homepage](#) for more

Download details:

IP Address: 129.252.86.83

The article was downloaded on 28/05/2010 at 16:29

Please note that [terms and conditions apply](#).

High-pressure behaviour of $\text{Li}_2\text{CaHfF}_8$ scheelite

Andrzej Grzechnik^{1,3}, Jean-Yves Gesland² and Karen Friese¹

¹ Departamento de Física de la Materia Condensada, Universidad del País Vasco, Apartado 644, Bilbao, E-48080, Spain

² Université du Maine-Cristallogénese, F-72025 Le Mans cedex, France

E-mail: andrzej@wm.lc.ehu.es

Received 8 January 2007

Published 14 February 2007

Online at stacks.iop.org/JPhysCM/19/096215

Abstract

High-pressure behaviour of $\text{Li}_2\text{CaHfF}_8$ scheelite ($I\bar{4}$, $Z = 2$) has been studied with synchrotron angle-dispersive powder and laboratory single-crystal x-ray diffraction using diamond anvil cells to 9.2 GPa at room temperature. The zero-pressure bulk modulus, its first pressure derivative, and the unit-cell volume at ambient pressure are $B_0 = 78(3)$ GPa, $B' = 4.42(64)$, and $V_0 = 273.67(19)$ Å³, respectively. The structural parameters obtained from the refinement of the single-crystal data show that all the polyhedra around the cations become more regular upon compression. The softest polyhedra are the CaF_8 units. Compared with previous investigations on LiMF_4 scheelites ($I4_1/a$, $Z = 4$; M: Y^{3+} , Gd^{3+} , or Lu^{3+}), in which the structural units most sensitive to increasing pressure are the LiF_4 tetrahedra, our observations indicate that the compressibility mechanism in fluoride scheelites depends on the cationic substitution and distribution.

(Some figures in this article are in colour only in the electronic version)

1. Introduction

Fluoride compounds LiMF_4 , in which M is a trivalent cation, have the scheelite structure ($I4_1/a$, $Z = 4$), that is a superstructure of fluorite CaF_2 ($Fm\bar{3}m$, $Z = 4$). The fluorine atoms are in a cubic arrangement and the Li^{1+} and M^{3+} cations are fourfold and eightfold coordinated with fluorines, respectively. A related group of materials is formed when the M^{3+} cation is replaced by divalent (M' : Ca or Cd) and tetravalent (M'' : Th, U, Ce, Tb, Zr, or Hf) cations to form a fully ordered scheelite-derived structure $\text{Li}_2\text{M}'\text{M}''\text{F}_8$ [1–3] (figure 1). Originally, Vedrine *et al* described Li_2CaUF_8 in space group $I\bar{4}$ ($Z = 2$) [1]. Later, they determined its space group to be $I\bar{4}m2$ ($Z = 2$) [2]. The sublattice formed by Li, Ca, and U atoms ($I\bar{4}m2$, $Z = 2$) is equivalent to that of LiYF_4 scheelite ($I4_1/a$, $Z = 4$), while the fluorine atoms are distributed in two half-occupied sites [2]. The structural models in space groups $I\bar{4}m2$ and

³ Author to whom any correspondence should be addressed.

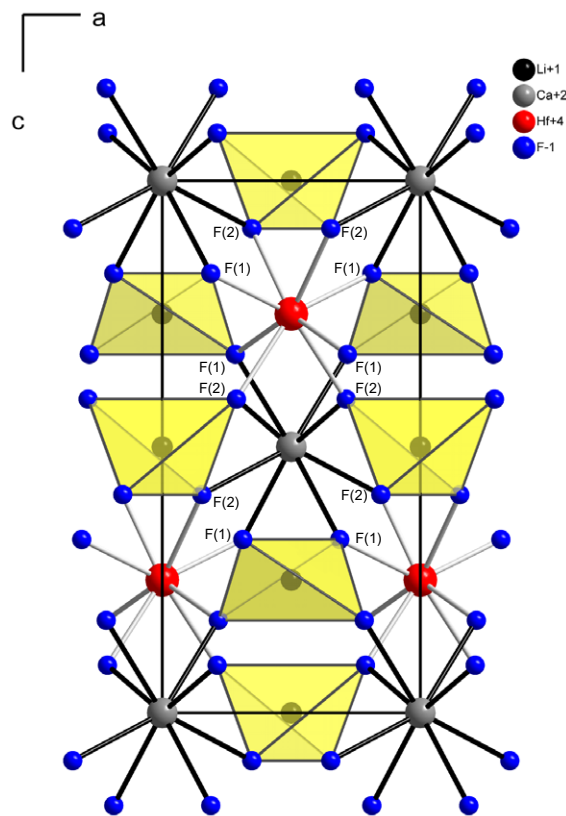


Figure 1. Crystal structure of $\text{Li}_2\text{CaHfF}_8$ ($I\bar{4}$, $Z = 2$). Some of the fluorine atoms are labelled.

$I\bar{4}$ are related through a group–subgroup relationship. Recently, the structure of $\text{Li}_2\text{CaHfF}_8$ has been determined in space group $I\bar{4}$ ($Z = 2$) [3] (figure 1). The $\text{Li}_2\text{M}'\text{M}''\text{F}_8$ model in $I\bar{4}$ ($Z = 2$) can be derived from the LiMF_4 one ($I4_1/a$, $Z = 4$) by removing the centre of symmetry and by distributing the M' and M'' cations in an ordered way over the two resulting M sites.

Previous experimental high-pressure investigations have shown that the actual behaviour of scheelite-structured LiMF_4 fluorides is closely related to the radii of the M^{3+} cations [4–6]. In LiYF_4 , in addition to the scheelite \rightarrow fergusonite ($I4_1/a \rightarrow I2/a$) transition at about 11 GPa, another structural transformation above 17 GPa to an as yet undetermined polymorph has been detected [4]. LiGdF_4 scheelite decomposes into a solid solution series $\text{Li}_y\text{Gd}_{1-y}\text{F}_{3-2y}$ ($P6_3/mmc$, $Z = 2$) and LiF above 11 GPa [5]. At 10.5 GPa, LiLuF_4 undergoes a tricritical phase transition to the fergusonite structure [6]. No other transformation occurs in lithium lutetium tetrafluoride up to 19.5 GPa. The zero-pressure bulk moduli of LiLuF_4 , LiYF_4 , and LiGdF_4 are 85(3), 81(4), and 76(4) GPa, respectively [4–6].

In this study, synchrotron angle-dispersive powder and laboratory single-crystal x-ray diffraction experiments on fully ordered $\text{Li}_2\text{CaHfF}_8$ scheelite ($I\bar{4}$, $Z = 2$) in diamond anvil cells at room temperature are reported. Its equation of state and pressure dependences of various structural parameters are determined and its compressibility mechanism is discussed in comparison to the high-pressure behaviour of simple LiYF_4 , LiGdF_4 , and LiLuF_4 scheelites ($I4_1/a$, $Z = 4$) [4–6].

2. Experimental details

A single crystal of $\text{Li}_2\text{CaHfF}_8$ was grown with the Czochralski method [3]. A part of it was finely ground and loaded into a diamond anvil cell for high-pressure angle-dispersive powder x-ray diffraction measurements to about 9.2 GPa on the Swiss–Norwegian Beamlines at the European Synchrotron Radiation Facility (BM1A, ESRF, Grenoble, France). Monochromatic radiation at 0.7100 Å was used for data collection on an image plate MAR345. The images were integrated with the program FIT2D [7] to yield intensity versus 2θ diagrams. The ruby luminescence method [8] was used for pressure calibration.

A series of x-ray single-crystal intensity measurements was performed at high pressure on another fragment of the same crystal (approximately $50 \times 50 \times 30 \mu\text{m}$) using a diffractometer IPDS-I (STOE) with Mo $K\alpha$ radiation. The diamond cell was of the Ahsbahs type (with the opening angle of 90°) [9]. The diamond culets ($600 \mu\text{m}$) were modified by laser machining so that the angle between them and the tapered parts of the diamonds was 40° . A $250 \mu\text{m}$ hole was drilled into a stainless steel gasket preindented to a thickness of $80 \mu\text{m}$. The intensities were collected upon compression. The data were measured in two different orientations of the diamond anvil cell rotated by 90° around the incident x-ray beam. For each of the orientations, the exposures were performed in the angular ranges $48^\circ \leq \varphi \leq 132^\circ$ and $228^\circ \leq \varphi \leq 312^\circ$. The integrated intensities were extracted and corrected for absorption using the STOE software⁴. Due to the particular semi-spherical cut of the diamonds, no absorption correction was necessary for the diamond anvils. Since a ruby luminescence system for pressure calibration was not available to us during our single-crystal measurements, the pressure was determined on the basis of the single-crystal lattice parameters from the equation of state obtained from the x-ray powder data (figure 2). Such a pressure calibration method has been discussed in [10]. The 1:4 mixture of ethanol:methanol was used as a hydrostatic pressure medium both during the powder and the single-crystal measurements.

3. Results and discussion

Figure 2 shows selected x-ray powder patterns at different pressure. The ambient-pressure lattice parameters and unit-cell volume of $\text{Li}_2\text{CaHfF}_8$ scheelite are $a_0 = 5.101(1) \text{ \AA}$, $c_0 = 10.513(1) \text{ \AA}$, and $V_0 = 273.55(14) \text{ \AA}^3$. The lattice parameters, unit-cell volumes, and c/a axial ratios do not show any anomaly that might be associated with a structural phase transition (figure 3). The compression data could be fitted up to 9.2 GPa by a Murnaghan equation of state, giving a zero-pressure bulk modulus $B_0 = 78(3) \text{ GPa}$ and a first pressure derivative of the bulk modulus $B' = 4.42(64)$ with $V_0 = 273.67(19) \text{ \AA}^3$. The bulk modulus for $\text{Li}_2\text{CaHfF}_8$ ($I\bar{4}$, $Z = 2$) is very similar to the moduli for LiMF_4 (M: Y^{3+} , Gd^{3+} , or Lu^{3+}) [4–6]. Of the four scheelites, $\text{Li}_2\text{CaHfF}_8$ is the most compressible along the c axis and its c/a axial ratio is the least sensitive to external pressure.

The refinements of the single-crystal data collected at 3.42 GPa have been made with the program JANA2000 [11]. Experimental data and structural parameters⁵ are given in tables 1 and 2. The two data sets for two different orientations of the diamond anvil cell have been refined together, but with two separate scale factors. The structural model in space group $I\bar{4}$ ($Z = 2$) consisted of the Li(1), Li(2), Ca, and Hf atoms at the positions $(0, 1/2, 1/4)$, $(0, 0, 1/2)$, $(0, 0, 0)$, and $(0, 1/2, 3/4)$, respectively [3]. The positions of the F atoms have been determined from the difference $F_{\text{obs}} - F_{\text{calc}}$ Fourier synthesis. The displacement parameters

⁴ TWIN and X-SHAPE. STOE & Cie GmbH, Darmstadt.

⁵ Further details of the crystallographic investigations can be obtained from the Fachinformationszentrum Karlsruhe, D-76344 Eggenstein-Leopoldshafen, Germany, on quoting the depository number CSD 417619.

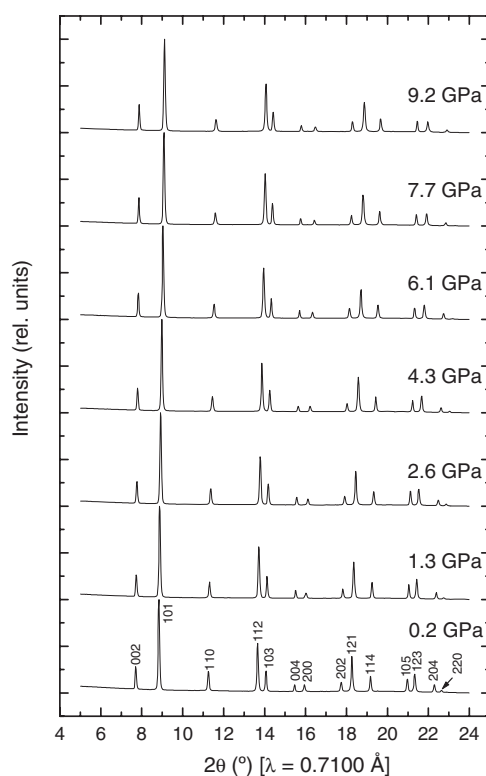


Figure 2. X-ray powder patterns of $\text{Li}_2\text{CaHfF}_8$ upon compression. Pressures are given in GPa. Miller indices mark the reflections of the scheelite.

of the Li atoms have not been refined. Of the remaining atoms, only the displacements parameters for the heaviest atom Hf have been refined anisotropically, as we have encountered problems with the anisotropic refinement of these parameters for the other atoms. We attribute this to the limited resolution of the data, i.e., the $\sin(\theta)/\lambda$ limit (table 1) is relatively low because of the small opening angle in our diamond anvil cell. An isotropic Gaussian extinction correction (G_{iso}) has also been applied [12].

As the acentric tetragonal space group allows for merohedral twinning of type I and II, the corresponding tests have been carried out using both an inversion centre and the additional mirror plane(s), which are in accordance with the holohedry of the tetragonal lattice as the twinning operations. No significant volume fractions of any of the twin orientations have been obtained from the refinement. An additional refinement of the enantiomorphic form of the crystal structure has led to overall agreement factors more than one per cent worse than the ones corresponding to the orientation given here (tables 1 and 2). This is of course due to the high f'' value for the Hf atom (6.1852) at the wavelength used (Mo $K\alpha$).

In the crystal structure of $\text{Li}_2\text{CaHfF}_8$, the Li(1) and Li(2) atoms are coordinated by the F(1) and F(2) atoms, respectively (figure 1, table 3). The four F(1) atoms are at a longer distance from the Ca^{2+} cations than the four F(2) atoms. On the other hand, the Hf–F(2) distances are longer than the Hf–F(1) distances. Unlike the Hf–F(2) bond length, the Hf–F(1) interatomic distance is constant upon compression (table 3). The relative changes in Li–F and Ca–F bond lengths are respectively similar. When pressure is increased, the volume of the $\text{Li}(1)\text{F}(1)_4$ tetrahedra [13] essentially does not change at all (table 4), while the most

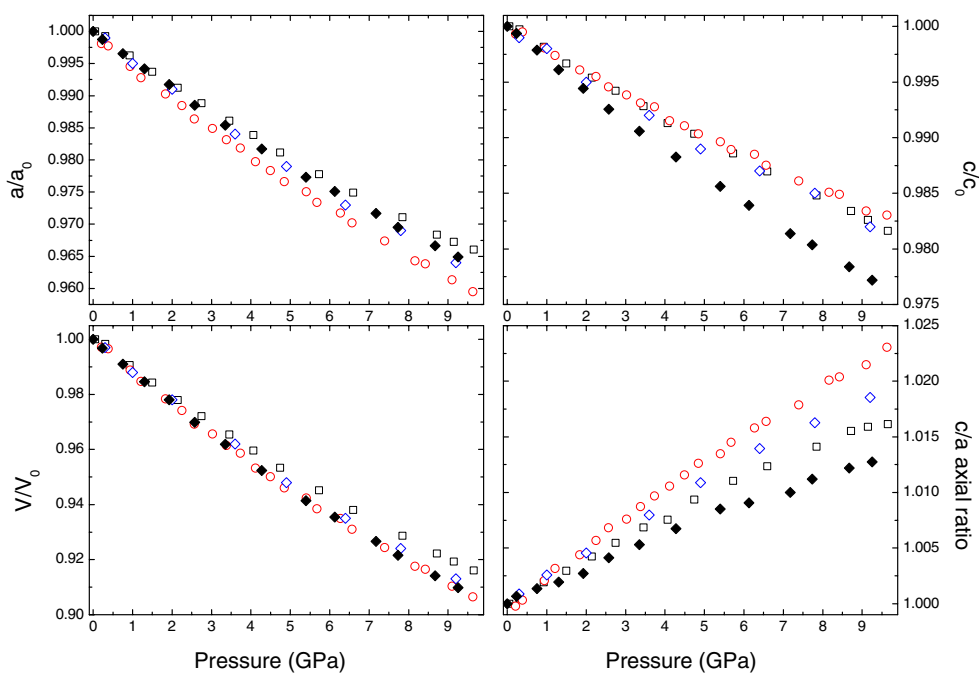


Figure 3. Lattice parameters, unit-cell volumes, and c/a axial ratios for $\text{Li}_2\text{CaHfF}_8$ (full symbols), normalized to the respective values at atmospheric pressure. They are compared with the high-pressure data for LiYF_4 [4] (open blue diamonds), LiGdF_4 [5] (open red circles), and LiLuF_4 [6] (open black squares).

compressible polyhedra are the CaF_8 units. Such a structural feature of this double scheelite is quite remarkable since the LiF_4 tetrahedra are softer than the YF_8 polyhedra in related LiYF_4 ($I4_1/a$, $Z = 4$) [4].

The polyhedral distortion parameters⁶ at different conditions are shown in table 5. The two inequivalent LiF_4 tetrahedra, substantially distorted at ambient conditions, behave in a distinct way (figure 1). The angular deformation of the $\text{Li}(2)\text{F}(2)_4$ tetrahedron practically does not change, while the $\text{Li}(1)\text{F}(1)_4$ tetrahedron becomes more regular. Correlated are the variations in the bond-length distortion parameters for the CaF_8 and HfF_8 polyhedra. Although the parameters for both structural units become smaller upon compression, it is the parameter for the HfF_8 polyhedra that is more sensitive to increased pressure.

The anisotropic compressibility (figure 3) could further be analysed when the F...F interatomic distances in the CaF_8 and HfF_8 polyhedra are considered (figure 4). The most striking feature is the elongation and shortening of the distances in the CaF_8 polyhedron perpendicular and along the c axis upon compression, respectively. The corresponding distances in the HfF_8 polyhedron are constant and become elongated, respectively. This result contrasts with what has already been observed in LiYF_4 scheelite, in which all the F...F distances diminish at high pressures [4].

The pressure evolution of structural distortions, especially in its anionic sublattice, of the polyhedral volumes, and of the anisotropic compressibility could also be elucidated by

⁶ The angular distortion of the LiF_4 tetrahedra is $100(|\alpha_1 - \alpha_0| + 2|\alpha_2 - \alpha_0|)/(3\alpha_0)$, where α_1 and α_2 are tetrahedral angles, while $\alpha_0 = 109.471^\circ$. The bond-length distortion of the XF_8 polyhedra is $100|d_1 - d_2|/|d_1 + d_2|$, where d_1 and d_2 are X-F(1) and X-F(2) distances (X: Ca or Hf), respectively.

Table 1. Experimental data for the single-crystal measurement at 3.42 GPa.

Crystal data	
a (Å)	5.032(1)
c (Å)	10.384(4)
V (Å ³)	262.9(2)
ρ (g cm ⁻³)	4.8542
μ (mm ⁻¹)	20.923
G_{iso}	0.039(5)
Data collection	
No. measured refl.	504
Range of hkl	$-5 \leq h \leq 5$ $-5 \leq k \leq 5$ $-10 \leq l \leq 10$
No. unique refl.	332
No. observed refl. ^a	280
$R(\text{int})_{\text{obs/all}}$ ^b	4.48/4.59
$\sin(\theta)/\lambda$	0.570 279
Refinement ^b	
R_{obs}	4.30
wR_{obs}	4.48
R_{all}	4.54
wR_{all}	4.64
GoF _{all}	0.95
GoF _{obs}	1.02
No. parameters	14

^a Criterion for observed reflections is $|F_{\text{obs}}| > 3\sigma$.

^b All agreement factors are given in %, weighting scheme $1/[\sigma^2(F_{\text{obs}}) + (0.01F_{\text{obs}})^2]$.

Table 2. Structural parameters from single-crystal refinements at 3.42 GPa.

Atom	x	y	z	U_{iso}
Li(1)	0	1/2	1/4	0.02
Li(2)	0	0	1/2	0.02
Ca	0	0	0	0.03(2)
Hf	0	1/2	3/4	0.009(1)
F(1)	0.312(2)	0.283(2)	0.674(1)	0.009(3)
F(2)	0.153(2)	0.712(2)	0.590(2)	0.017(3)

Table 3. Interatomic distances (Å) at 3.42 GPa compared with the ones at atmospheric pressure [3] (italics). The estimated standard deviations are given in brackets.

Atoms	Li(1)	Li(2)	Ca	Hf
F(1)	<i>1.905</i> 1.882(12)		2.377 2.314(14)	2.067 2.070(12)
F(2)		<i>1.901</i> 1.885(14)	2.307 2.249(13)	2.140 2.123(15)

pseudosymmetry that is indicative of a slightly distorted structure of higher symmetry. If the distortion is small enough, it can be expected that the material would tend to acquire the more symmetric structure as a function of pressure and/or temperature [14]. For this purpose, we have used the program PSEUDO of the Bilbao Crystallographic Server [15]. The program

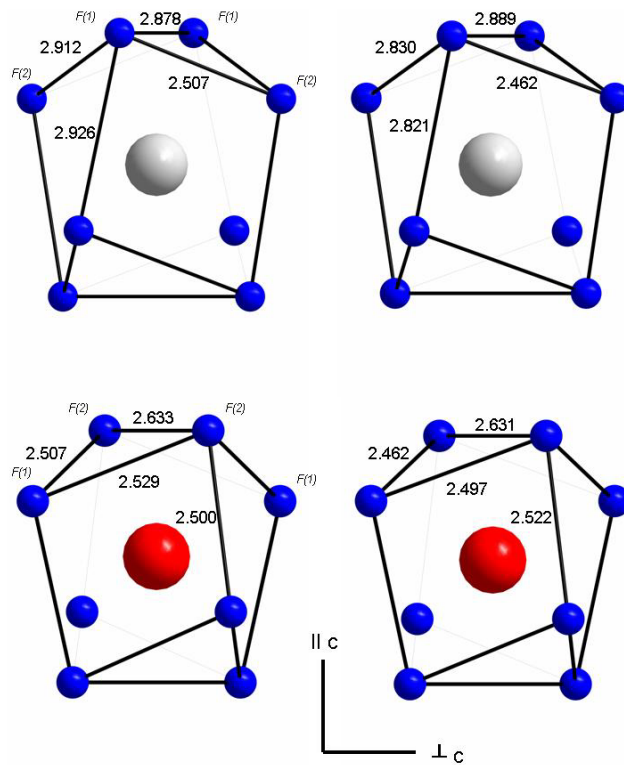


Figure 4. CaF_8 (top) and HfF_8 (bottom) polyhedra at ambient conditions (left) and at 3.42 GPa (right). The unique axis is vertical. The symbols label the F atoms. The numbers stand for the F...F distances. The legends of the atoms are given in figure 1.

Table 4. Comparison of the polyhedral volumes (\AA^3) at atmospheric conditions (V_0) [3] and at 3.42 GPa (V).

Polyhedra	Ambient pressure	3.42 GPa	Volume ratio (V/V_0)
$\text{Li}(1)\text{F}(1)_4$	3.04(2)	3.07(5)	1.01
$\text{Li}(2)\text{F}(2)_4$	3.43(3)	3.34(6)	0.97
CaF_8	22.43(11)	20.76(23)	0.93
HfF_8	16.60(9)	16.38(2)	0.99

Table 5. Comparison of the distortion parameters for the LiF_4 , CaF_8 , and HfF_8 polyhedra at atmospheric conditions (D_0) [3] and at 3.42 GPa (D).

Polyhedra	Ambient pressure	3.42 GPa	Ratio D/D_0
$\text{Li}(1)\text{F}(1)_4$	14.09	12.08	0.86
$\text{Li}(2)\text{F}(2)_4$	6.50	6.70	1.03
CaF_8	1.50	1.42	0.95
HfF_8	1.74	1.34	0.71

works in two steps: (1) it calculates all the minimal supergroups of a given space group, (2) it calculates the displacements of the atoms that are necessary to obtain a higher symmetry structure with the symmetry of the chosen minimal supergroup. $\text{Li}_2\text{CaHfF}_8$ shows pronounced

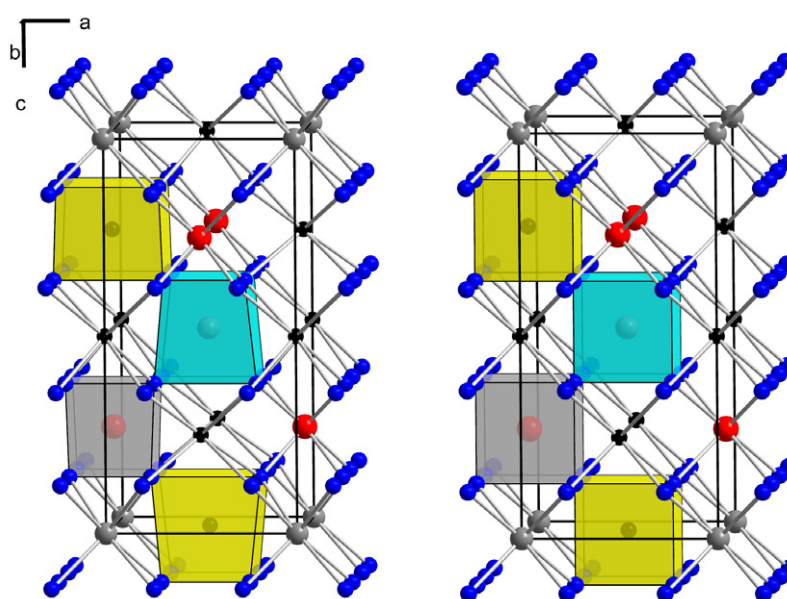


Figure 5. Crystal structure of the pseudosymmetrical phase ($I\bar{4}m2$, $Z = 2$) at 3.42 GPa with the average fluorine coordinates of table 6 (left) and with the ideal fluorite-like coordinates (right). The legends of the atoms are given in figure 1.

Table 6. Fractional coordinates of the F atom in space group $I\bar{4}m2$ at ambient conditions [3] and at 3.42 GPa.

Coordinates	Ambient pressure	3.42 GPa
x	0.288	0.286
y	0.230	0.232
z	0.365	0.368

pseudosymmetry with respect to the space group $I\bar{4}m2$, the minimal supergroup of $I\bar{4}$, that was reported for related disordered Li_2CaUF_8 scheelite [2]. In fact, the fully ordered cationic substructure of $\text{Li}_2\text{CaHfF}_8$ is in accordance with the symmetry of space group $I\bar{4}m2$, and it is only the fluorine ions that reduce the symmetry to $I\bar{4}$. In pseudosymmetrical supergroup $I\bar{4}m2$, the Li(1), Li(2), Ca, and Hf cations are at the Wyckoff sites 2c, 2b, 2a, and 2d, respectively, while the fluorine atoms are all at the fully occupied general position 16j. The resulting structure is of the distorted fluorite type, in which all the cations are surrounded by eight fluorines at the vertices of deformed cubes (figure 5). Table 6 shows the fractional coordinates of the F atom in $I\bar{4}m2$ resulting from the displacement of the initial F(1) and F(2) atoms in $I\bar{4}$ (figure 1) using the pseudosymmetry approach. These coordinates do not deviate much from the ideal values (0.25, 0.25, 0.375), for which all the polyhedra around the cations are undistorted cubes like in the ideal fluorite-type structure (figure 5). The maximum displacements (their absolute values are in Å) of the F(1) and F(2) atoms necessary to obtain the higher symmetrical structure are shown in table 7.⁷ All of them are bigger at ambient pressure than at 3.42 GPa. The largest relative change in the displacements on compression to 3.42 GPa is along the c axis ($\Delta z_{3.42 \text{ GPa}}/\Delta z_{\text{ambient}} \sim 92\%$).

⁷ The displacements along the a and b axes are permutable.

Table 7. Displacements of the F(1) and F(2) atoms (in Å) in space group $I\bar{4}$ necessary to obtain the pseudosymmetrical $I\bar{4}m2$ structure at ambient conditions [3] and at 3.42 GPa.

Displacements	Ambient conditions	3.42 GPa
Δx	± 0.425	± 0.400
Δy	± 0.002	± 0.013
Δz	± 0.473	± 0.436
Total	0.636	0.592

4. Conclusions

Our observations demonstrate that the distortions and the pseudosymmetry of the fluorite-derived $\text{Li}_2\text{CaHfF}_8$ scheelite structure in space group $I\bar{4}$ ($Z = 2$) are pressure dependent. The largest and the most pressure-sensitive distortions of the ideal fluorite aristotype occur along the c axis, while all the polyhedra around the cations become more regular upon compression.

It has previously been found that the c/a ratio increases in LiYF_4 scheelite ($I4_1/a$, $Z = 4$) at high pressures because of large compressibility of the tetrahedral units LiF_4 [4]. On the other hand, when the eightfold-coordinated polyhedra are more compressible, e.g., in tungstate scheelites [16, 17], this ratio decreases. In the case of $\text{Li}_2\text{CaHfF}_8$, the combined effect of large and low compressibilities of the CaF_8 and HfF_8 polyhedra, respectively, thus leads to the relative insensitivity of its c/a ratio upon compression (figure 3). This implies that the pressure dependence of the c/a axial ratio in fluoride scheelites is strongly affected by the polyhedral compressibilities and distortions around the heavy cations present in the structure.

Acknowledgments

The x-ray powder data were collected during the HS-2347 beamtime at the European Synchrotron Radiation Facility (Grenoble). Experimental assistance from the staff of the Swiss–Norwegian Beamlines at ESRF is gratefully acknowledged. We thank Alberto Herrero (TEKNIKER, Eibar) for his help with preparations of the measurements in our high-pressure laboratory. This work has been financially supported by the Ministerio de Ciencia y Tecnología and the Gobierno Vasco.

References

- [1] Vedrine A, Baraduc L and Cousseins J C 1973 *Mater. Res. Bull.* **8** 581
- [2] Vedrine A, Trottier D, Cousseins J C and Chevalier R 1979 *Mater. Res. Bull.* **14** 583
- [3] Ayala A P, Paschoal C W A, Gesland J-Y, Ellena J, Castellano E E and Moreira R L 2002 *J. Phys.: Condens. Matter* **14** 5485
- [4] Grzechnik A, Syassen K, Loa I, Hanfland M and Gesland J Y 2002 *Phys. Rev. B* **65** 104102
- [5] Grzechnik A, Crichton W A, Bouvier P, Dmitriev V, Weber H-P and Gesland J-Y 2004 *J. Phys.: Condens. Matter* **16** 7779
- [6] Grzechnik A, Friese K, Dmitriev V, Weber H-P, Gesland J-Y and Crichton W A 2005 *J. Phys.: Condens. Matter* **17** 763
- [7] Hammersley A P, Svensson S O, Hanfland M, Fitch A N and Häusermann D 1996 *High Pressure Res.* **14** 235
- [8] Piermarini G J, Block S, Barnett J D and Forman R A 1975 *J. Appl. Phys.* **46** 2774
- [9] Mao H K, Xu J and Bell P M 1986 *J. Geophys. Res.* **91** 4673
- [9] Ahsbahs H 1995 *Z. Kristallogr. Suppl.* **9** 42
- [9] Ahsbahs H 2004 *Z. Kristallogr.* **219** 305
- [10] Grzechnik A, Balic-Zunic T, Makovicky E, Gesland J-Y and Friese K 2006 *J. Phys.: Condens. Matter* **18** 2915

-
- [11] Petricek V, Dusek M and Palatinus L 2000 *Jana2000. The Crystallographic Computing System* (Praha: Institute of Physics)
- [12] Becker P J and Coppens P 1974 *Acta Crystallogr. A* **30** 129
- [13] Balic-Zunic T and Vickovic I 1996 *J. Appl. Crystallogr.* **29** 305
- [14] Kroumova E, Aroyo M I and Perez-Mato J M 2002 *Acta Crystallogr. B* **58** 921
- [15] <http://www.cryst.ehu.es/>
Kroumova E, Aroyo M I, Perez-Mato J M, Ivantchev S, Igartua J M and Wondratschek H 2001 *J. Appl. Crystallogr.* **34** 783
- [16] Hazen R M, Finger L W and Mariathasan J W E 1985 *J. Phys. Chem. Solids* **46** 253
- [17] Grzechnik A, Crichton W A, Marshall W G and Friese K 2006 *J. Phys.: Condens. Matter* **18** 3017